6th European Conference on Computational Mechanics (ECCM 6)
7th European Conference on Computational Fluid Dynamics (ECFD 7)
1115 June 2018, Glasgow, UK

A MIXED VARIATIONAL FRAMEWORK FOR NON-LINEAR ELECTRO-ELASTODYNAMICS

Alexander Janz[1], Peter Betsch[1], Marlon Franke[1], Rogelio Ortigosa[2] and Antonio J. Gil[2]

[1] Institute of Mechanics, Karlsruhe Institute of Technology
76131 Karlsruhe, Germany
{alexander.janz, peter.betsch, marlon.franke}@kit.edu;
https://www.ifm.kit.edu/english/14.php

[2] Zienkiewicz Centre for Computational Engineering, College of Engineering, Swansea University
Bay Campus, SA1 8EN, United Kingdom
{r.ortigosa, a.j.gil}@swansea.ac.uk; http://www.swansea.ac.uk/staff/engineering/

Key words: Non-linear electro-elastodynamics, energy-momentum scheme, mixed variational framework, multi-convexity, mixed finite elements

Abstract. The present work deals with a mixed approach to the design of energy and momentum (EM) consistent integration schemes in the field of non-linear electro-elastodynamics

1 Introduction

The importance of electro-active polymers (EAPs) in different applications such as actuators and sensors, soft robotics or artificial muscles require advanced simulation techniques to prognosticate the behavior of such smart materials. Typically, these materials are described static from the electrical standpoint and dynamic from the mechanical standpoint. Thus, a consistent, stable and accurate time integration of the electro-elasto-dynamical equations is fundamental for modelling purposes. In this work we present a new approach to the design of energy-momentum (EM) consistent algorithms inspired by the structure of polyconvex internal energy functions (see [1]) and tailor-made for the consistent space-time discretization of EAPs. A Hu-Washizu-type mixed variational framework with a novel cascade form of kinematic constraints [2] along with the concept of partitioned discrete derivatives [3] leads to a structure-preserving time integrator, which shows superior numerical stability and

robustness (see [4], or in case of thermo-elastodynamics [5]) compared to alternative formulations. This work can be seen as an extension of [4] to mixed formulations in the sense of [2]. Note that the mixed framework makes possible a wide variety of finite element formulations.

2 Continuum electro-elastodynamics

The present section provides a summary of non-linear continuum electromechanics and the governing equations without claim of completeness (for more details consider e.g. [6] and the references therein).

2.1 Kinematics

An EAP modeled as a deformable body $\mathcal{B}$ with boundary $\partial\mathcal{B}$ placed in its reference configuration $\mathcal{B}_0 \in \mathbb{R}^3$ and its current configuration $\mathbb{R}^3 \ni \mathcal{B}_t = \boldsymbol{\varphi}(\mathcal{B}_0, t)$ is considered within time $t \in \mathcal{I} = [0, T]$, where $T \in \mathbb{R}^+$. The material configuration is given by $\mathbf{X} = X_A \, \mathbf{E}_A$ with material basis $\mathbf{E}_A$ and corresponding coordinates X_A, $A = 1, 2, 3$. The bijective mapping $\boldsymbol{\varphi} : \mathcal{B}_0 \times \mathcal{I} \to \mathbb{R}^3$ maps a material point $\mathbf{X}$ to its current placement $\mathbf{x} = x_a \, \mathbf{e}_a$ which is relative to the basis $\mathbf{e}_a$ and corresponding coordinates x_a, $a = 1, 2, 3$. In particular the current position of $\mathbf{X}$ is given by the deformation field

$$\mathbf{x} = \boldsymbol{\varphi} := \boldsymbol{\varphi}(\mathbf{X}, t) \,, \tag{1}$$

where deformations are prescribed by $\bar{\boldsymbol{\varphi}} : \partial_{\boldsymbol{\varphi}}\mathcal{B}_0 \times \mathcal{I} \to \mathbb{R}^3$ on a portion $\partial_{\boldsymbol{\varphi}}\mathcal{B}_0 \subset \partial\mathcal{B}_0$. The material velocity field $\mathbf{V} : \mathcal{B}_0 \times \mathcal{I} \to \mathbb{R}^3$ at time t is given by $\mathbf{V} := \dot{\boldsymbol{\varphi}}$. The superposed dot denotes the material differentiation with respect to time. The deformation gradient is a second-order two-point tensor field $\mathbf{F}_{\boldsymbol{\varphi}} : \mathcal{B}_0 \times \mathcal{I} \to \mathbb{R}^{3\times3}$ given by

$$\mathbf{F}_{\boldsymbol{\varphi}} = \nabla\boldsymbol{\varphi} \,, \tag{2}$$

where ∇ represents the material gradient operator, defined as $\nabla(\bullet) = \frac{\partial(\bullet)}{\partial\mathbf{X}}$. The deformation gradient maps infinitesimal vectors $\mathrm{d}\mathbf{X}$ placed at $\mathbf{X} \in \mathcal{B}_0$ to the corresponding infinitesimal spatial line element $\mathrm{d}\mathbf{x}$ placed at $\mathbf{x} \in \mathcal{B}_t$ as $\mathrm{d}\mathbf{x} = \mathbf{F}_{\boldsymbol{\varphi}} \, \mathrm{d}\mathbf{X}$. An infinitesimal material area element can be computed using the cross product of two linearly independent line elements $\mathrm{d}\mathbf{X}_1$ and $\mathrm{d}\mathbf{X}_2$ placed at $\mathbf{X} \in \mathcal{B}_0$, such that $\mathrm{d}\mathbf{A} = \mathrm{d}\mathbf{X}_1 \times \mathrm{d}\mathbf{X}_2$. Thus the corresponding spatial area element placed at $\mathbf{x} \in \mathcal{B}_t$ is given by $\mathrm{d}\mathbf{a} = \mathrm{d}\mathbf{x}_1 \times \mathrm{d}\mathbf{x}_2 = (\mathbf{F}_{\boldsymbol{\varphi}} \, \mathrm{d}\mathbf{X}_1) \times (\mathbf{F}_{\boldsymbol{\varphi}} \, \mathrm{d}\mathbf{X}_2) = \mathbf{H}_{\boldsymbol{\varphi}} \, \mathrm{d}\mathbf{A}$. Here, $\mathbf{H}_{\boldsymbol{\varphi}} : \mathcal{B}_0 \times \mathcal{I} \to \mathbb{R}^{3\times3}$ denotes the cofactor of $\mathbf{F}_{\boldsymbol{\varphi}}$, thus

$$\mathbf{H}_{\boldsymbol{\varphi}} = \mathrm{cof}(\mathbf{F}_{\boldsymbol{\varphi}}) = \frac{1}{2} \, \mathbf{F}_{\boldsymbol{\varphi}} \overset{\bullet}{\times} \mathbf{F}_{\boldsymbol{\varphi}}; \qquad (H_{\boldsymbol{\varphi}})_{iI} = \frac{1}{2} \, \varepsilon_{ijk} \, \varepsilon_{IJK} \, (F_{\boldsymbol{\varphi}})_{jJ} \, (F_{\boldsymbol{\varphi}})_{kK} \,, \tag{3}$$

where ε_{ijk} denotes the permutation symbol and the summation convention applies to pairs of repeated indices. Similarly an infinitesimal material volume element placed at $\mathbf{X} \in \mathcal{B}_0$ can be computed employing three non-coplanar infinitesimal material line elements $\mathrm{d}\mathbf{X}_1$, $\mathrm{d}\mathbf{X}_2$ and $\mathrm{d}\mathbf{X}_3$ which in particular form a positive triad such that $\mathrm{dV} = \big(\mathrm{d}\mathbf{X}_1 \times \mathrm{d}\mathbf{X}_2\big) \cdot \mathrm{d}\mathbf{X}_3 > 0$ .Accordingly, the corresponding infinitesimal spatial volume element placed at $\mathbf{x} \in \mathcal{B}_t$ yields $\mathrm{dv} = \big(\mathrm{d}\mathbf{x}_1 \times \mathrm{d}\mathbf{x}_2\big) \cdot \mathrm{d}\mathbf{x}_3 = \det(\mathbf{F}_{\boldsymbol{\varphi}})\ \mathrm{dV} = J_{\boldsymbol{\varphi}}\ \mathrm{dV}$, where the Jacobian determinant $J_{\boldsymbol{\varphi}} : \mathcal{B}_0 \times \mathcal{I} \to \mathbb{R}^+$ is defined by

$$J_{\boldsymbol{\varphi}} = \det(\mathbf{F}_{\boldsymbol{\varphi}}) = \frac{1}{6}\, \mathbf{F}_{\boldsymbol{\varphi}} \maltese \mathbf{F}_{\boldsymbol{\varphi}} : \mathbf{F}_{\boldsymbol{\varphi}} = \frac{1}{3}\, \mathbf{H}_{\boldsymbol{\varphi}} : \mathbf{F}_{\boldsymbol{\varphi}}; \qquad J_{\boldsymbol{\varphi}} = \frac{1}{3}\, (H_{\boldsymbol{\varphi}})_{iI}\, (F_{\boldsymbol{\varphi}})_{iI}\,. \tag{4}$$

In the above, the tensor cross product operator as introduced in [7] and reused in the context of continuum mechanics by [8] has been used. Note that the expressions of $\mathbf{H}_{\boldsymbol{\varphi}}$ and $J_{\boldsymbol{\varphi}}$ lead to a great simplification of the formulation in terms of their directional derivatives and in the design of EM schemes.

2.2 Finite strain electro-elastodynamics

The local form of balance of linear momentum can be stated as

$$\begin{aligned} \rho_0 \dot{\mathbf{V}} - \mathrm{DIV}\,(\mathbf{F}_{\boldsymbol{\varphi}}\mathbf{S}) - \bar{\mathbf{B}} &= \mathbf{0}; && \text{in } \mathcal{B}_0; \\ (\mathbf{F}_{\boldsymbol{\varphi}}\mathbf{S})\,\mathbf{N} &= \bar{\mathbf{T}}; && \text{on } \partial_{\boldsymbol{P}}\mathcal{B}_0; \\ \boldsymbol{\varphi} &= \bar{\boldsymbol{\varphi}}; && \text{on } \partial_{\boldsymbol{\varphi}}\mathcal{B}_0, \end{aligned} \tag{5}$$

where $\rho_0 : \mathcal{B}_0 \to \mathbb{R}_+$ represents the reference mass density field, $\bar{\mathbf{B}} : \mathcal{B}_0 \times \mathcal{I} \to \mathbb{R}^3$ are prescribed body forces and $\bar{\mathbf{T}} : \partial_{\boldsymbol{P}}\mathcal{B}_0 \times \mathcal{I} \to \mathbb{R}^3$ are prescribed stresses on $\partial_{\boldsymbol{P}}\mathcal{B}_0 \subset \partial\mathcal{B}_0$. As usual, we have the standard relationships $\partial\mathcal{B}_0 = \partial_{\boldsymbol{P}}\mathcal{B}_0 \cup \partial_{\boldsymbol{\varphi}}\mathcal{B}_0$ and $\partial_{\boldsymbol{P}}\mathcal{B}_0 \cap \partial_{\boldsymbol{\varphi}}\mathcal{B}_0 = \varnothing$. Furthermore, $\mathbf{S}$ denotes the second Piola-Kirchhoff stress tensor and $\mathbf{N}$ the unit outward normal vector acting on $\mathbf{X} \in \partial\mathcal{B}_0$. The partial differential equation and boundary conditions in (5) have to be supplemented with suitable initial configurations provided by $\boldsymbol{\varphi}(\mathbf{X}, 0) = \boldsymbol{\varphi}_0$ and $\mathbf{V}(\mathbf{X}, 0) = \mathbf{V}_0$.

Based on the assumptions that magnetic and time-dependent effects can be neglected, Maxwell equations reduce to the laws stated by Gauss and Faraday [6]. The local form of Gauss law in the Lagrangian setting can be stated as

$$\begin{aligned} \mathrm{DIV}\mathbf{D} - \rho_0^e &= 0; && \text{in } \mathcal{B}_0; \\ \mathbf{D} \cdot \mathbf{N} &= -\omega_0^e; && \text{on } \partial_{\omega}\mathcal{B}_0, \end{aligned} \tag{6}$$

using the Lagrangian electric displacement vector $\mathbf{D} : \mathcal{B}_0 \times \mathcal{I} \to \mathbb{R}^3$, an electric charge per unit undeformed volume $\rho_0^e : \mathcal{B}_0 \times \mathcal{I} \to \mathbb{R}$ and an electric surface charge per unit

of undeformed area $\omega_0^e : \partial_\omega \mathcal{B}_0 \times \mathcal{I} \to \mathbb{R}$ on $\partial_\omega \mathcal{B}_0 \subset \partial \mathcal{B}_0$. Furthermore, the local form of Faraday's law in the Lagrangian setting is given by

$$\begin{aligned} \mathbf{E} &= -\nabla \phi; && \text{in } \mathcal{B}_0; \\ \phi &= \bar{\phi}; && \text{on } \partial_\phi \mathcal{B}_0, \end{aligned} \tag{7}$$

with the Lagrangian electric field vector $\mathbf{E} : \mathcal{B}_0 \times \mathcal{I} \to \mathbb{R}^3$ and the scalar electric potential $\phi : \mathcal{B}_0 \times \mathcal{I} \to \mathbb{R}$. Here $\bar{\phi} : \partial_\phi \mathcal{B}_0 \to \mathbb{R}$ are prescribed electrical potentials on $\partial_\phi \mathcal{B}_0 \subset \partial \mathcal{B}_0$. Similar to the mechanical boundaries, we have the standard relationships $\partial_\omega \mathcal{B}_0 \cup \partial_\phi \mathcal{B}_0 = \partial \mathcal{B}_0$ and $\partial_\omega \mathcal{B}_0 \cap \partial_\phi \mathcal{B}_0 = \varnothing$. Eventually, suitable initial conditions for the electrical potential are provided as $\phi(\mathbf{X}, 0) = \phi_0$.

2.3 Constitutive equations in non-linear electro-elasticity

To describe finite strain electro-elastodynamics an internal energy density per unit undeformed volume $\tilde{u} : \mathbb{R}^{3\times3} \times \mathbb{R}^3 \to \mathbb{R}$ is defined by the deformation gradient and the electrical displacement field as

$$\tilde{u}(\mathbf{F}_{\boldsymbol{\varphi}}, \mathbf{D}) = u(\mathbf{C}_{\boldsymbol{\varphi}}, \mathbf{D}) = \mathbb{U}(\mathbf{C}_{\boldsymbol{\varphi}}, \mathbf{G}_{\boldsymbol{\varphi}}, C_{\boldsymbol{\varphi}}, \mathbf{D}) \,, \tag{8}$$

which is assumed to be twice continuously differentiable with respect to its arguments. The frame-indifferent formulation of the internal energy density (8) has originally been introduced in [1]. Moreover, $\mathbb{U}(\mathbf{C}_{\boldsymbol{\varphi}}, \mathbf{G}_{\boldsymbol{\varphi}}, C_{\boldsymbol{\varphi}}, \mathbf{D}) : \mathbb{R}^{3\times3} \times \mathbb{R}^{3\times3} \times]0, +\inf[\times \mathbb{R}^3 \to \mathbb{R}$ is inspired by the important notion of polyconvexity where the symmetric kinematic quantities are the right Cauchy-Green strain tensor $\mathbf{C}_{\boldsymbol{\varphi}} : \mathcal{B}_0 \times \mathcal{I} \to \mathbb{R}^{3\times3}$, its cofactor $\mathbf{G}_{\boldsymbol{\varphi}} : \mathcal{B}_0 \times \mathcal{I} \to \mathbb{R}^{3\times3}$ and its determinant $C_{\boldsymbol{\varphi}} : \mathcal{B}_0 \times \mathcal{I} \to \mathbb{R}$ given by

$$\mathbf{C}_{\boldsymbol{\varphi}} = \mathbf{F}_{\boldsymbol{\varphi}}^{\mathrm{T}} \mathbf{F}_{\boldsymbol{\varphi}}; \quad \mathbf{G}_{\boldsymbol{\varphi}} = \operatorname{cof}(\mathbf{C}_{\boldsymbol{\varphi}}) = \frac{1}{2} \mathbf{C}_{\boldsymbol{\varphi}} \diamondsuit \mathbf{C}_{\boldsymbol{\varphi}}; \quad C_{\boldsymbol{\varphi}} = \det(\mathbf{C}_{\boldsymbol{\varphi}}) = \frac{1}{3} \mathbf{C}_{\boldsymbol{\varphi}} : \mathbf{G}_{\boldsymbol{\varphi}} \,. \tag{9}$$

The directional derivative of the internal energy with respect to its arguments yields the following relations

$$\mathrm{D}u\,(\mathbf{C}_{\boldsymbol{\varphi}}, \mathbf{D})\,[\delta\boldsymbol{\varphi}] = \mathbf{S} : \frac{1}{2}\mathrm{D}\mathbf{C}[\delta\boldsymbol{\varphi}]; \qquad \mathrm{D}u\,(\mathbf{C}_{\boldsymbol{\varphi}}, \mathbf{D})\,[\delta\mathbf{D}] = \mathbf{E} \cdot \delta\mathbf{D} \,. \tag{10}$$

The directional derivative of $\mathbb{U}$ with respect to the deformation and electrical displacement field, assume the form

$$\begin{aligned} \mathrm{D}\mathbb{U}[\delta\boldsymbol{\varphi}] &= \partial_{\boldsymbol{C}}\mathbb{U} : \mathrm{D}\mathbf{C}_{\boldsymbol{\varphi}}[\delta\boldsymbol{\varphi}] + \partial_{\boldsymbol{G}}\mathbb{U} : \mathrm{D}\mathbf{G}_{\boldsymbol{\varphi}}[\delta\boldsymbol{\varphi}] + \partial_{C}\mathbb{U}\,\mathrm{D}C_{\boldsymbol{\varphi}}[\delta\boldsymbol{\varphi}]; \\ \mathrm{D}\mathbb{U}[\delta\mathbf{D}] &= \partial_{\boldsymbol{D}}\mathbb{U} \cdot \delta\mathbf{D} \,, \end{aligned} \tag{11}$$

where the directional derivatives of the kinematic quantities are given by

$$\begin{aligned} \mathrm{D}\mathbf{C}_{\boldsymbol{\varphi}}[\delta\boldsymbol{\varphi}] &= (\nabla\delta\boldsymbol{\varphi})^{\mathrm{T}}\,\nabla\boldsymbol{\varphi} + (\nabla\boldsymbol{\varphi})^{\mathrm{T}}\,\nabla\delta\boldsymbol{\varphi}; \\ \mathrm{D}\mathbf{G}_{\boldsymbol{\varphi}}[\delta\boldsymbol{\varphi}] &= \mathbf{C}_{\boldsymbol{\varphi}} \diamond \mathrm{D}\mathbf{C}_{\boldsymbol{\varphi}}[\delta\boldsymbol{\varphi}]; \\ \mathrm{D}C_{\boldsymbol{\varphi}}[\delta\boldsymbol{\varphi}] &= \mathbf{G}_{\boldsymbol{\varphi}} : \mathrm{D}\mathbf{C}_{\boldsymbol{\varphi}}[\delta\boldsymbol{\varphi}]\,, \end{aligned} \tag{12}$$

see [2]. Inserting equations (12) in (11) and comparison with (10) an expression of the second Piola Kirchhoff stress tensor $\mathbf{S}$ and the electrical field vector $\mathbf{E}$ are given by

$$\mathbf{S} = 2\partial_{\boldsymbol{C}}\mathbb{U} + 2\partial_{\boldsymbol{G}}\mathbb{U} \diamond \mathbf{C}_{\boldsymbol{\varphi}} + 2\partial_{C}\mathbb{U}\mathbf{G}_{\boldsymbol{\varphi}}; \qquad \mathbf{E} = \partial_{\boldsymbol{D}}\mathbb{U}. \tag{13}$$

Example: In this work we decomposed the internal energy into a pure mechanical component and a coupled electro-mechanical component as $u(\mathbf{C}_{\boldsymbol{\varphi}}, \mathbf{D}) = u_m(\mathbf{C}_{\boldsymbol{\varphi}}) + u_{em}(\mathbf{C}_{\boldsymbol{\varphi}}, \mathbf{D})$, see [9]. For the pure mechanical contribution we consider a material response of a compressible Mooney-Rivlin model, given by

$$u_m^{MR}(\mathbf{C}_{\boldsymbol{\varphi}}) = \mathbb{U}_m^{MR}(\mathbf{C}_{\boldsymbol{\varphi}}, \mathbf{G}_{\boldsymbol{\varphi}}, C_{\boldsymbol{\varphi}}) = \frac{\mu_1}{2}\mathrm{tr}\mathbf{C}_{\boldsymbol{\varphi}} + \frac{\mu_2}{2}\mathrm{tr}\mathbf{G}_{\boldsymbol{\varphi}} - (\mu_1 + 2\mu_2)\ln C_{\boldsymbol{\varphi}}^{1/2} - \frac{\lambda}{2}\left(C_{\boldsymbol{\varphi}}^{1/2} - 1\right)^2, \tag{14}$$

where $\mu_1, \mu_2, \lambda \geq 0$ are material constants. Moreover, we focus on ideal dielectric elastomers, where the coupled part of the internal energy is given by

$$u_{em}(\mathbf{C}_{\boldsymbol{\varphi}}, \mathbf{D}) = \mathbb{U}_{em}(\mathbf{C}_{\boldsymbol{\varphi}}, C_{\boldsymbol{\varphi}}, \mathbf{D}) = \frac{1}{2\,\varepsilon_r\,\varepsilon_0\,C^{1/2}}\,\mathbf{D}\cdot\mathbf{C}_{\boldsymbol{\varphi}}\,\mathbf{D}\,, \tag{15}$$

with the vacuum permittivity ε_0 and the relative material permittivity ε_r.

3 Mixed variational framwork

In this section we present a new mixed variational formulation that lays the foundation for the energy-momentum consistent discretization approach developed in the sequel. In our approach, we introduce the fields $\mathbf{C}(\mathbf{X})$, $\mathbf{G}(\mathbf{X})$ and $C(\mathbf{X})$ as independent quantities. In particular, consider the cascade form of kinematic relationships as proposed in [2]:

$$\mathbf{C} = \nabla\boldsymbol{\varphi}^{\mathrm{T}}\,\nabla\boldsymbol{\varphi}; \quad \mathbf{G} = \frac{1}{2}\,\mathbf{C}\diamond\mathbf{C}; \quad C = \frac{1}{3}\,\mathbf{C} : \mathbf{G}\,. \tag{16}$$

The above relations can be viewed as kinematic constraints that link the strain-type quantities $\mathbf{C} \in \mathbb{V}_{\mathbf{C}}$, $\mathbf{G} \in \mathbb{V}_{\mathbf{G}}$ and $C \in \mathbb{V}_C$ to the deformation $\boldsymbol{\varphi} \in \mathcal{C}_{\boldsymbol{\varphi}}$. In this connection,

we introduce the sets

$$\begin{aligned}
\mathcal{C}_{\boldsymbol{\varphi}} &= \{\boldsymbol{\varphi} : \mathcal{B}_0 \times \mathcal{I} \to \mathbb{R}^3 \mid \text{ for } \varphi_i \in H^1(\mathcal{B}_0), \det(\nabla\boldsymbol{\varphi}) > 0 \;\forall \mathbf{X} \in \mathcal{B}_0,\; \boldsymbol{\varphi} = \bar{\boldsymbol{\varphi}} \;\forall \mathbf{X} \in \partial_{\boldsymbol{\varphi}}\mathcal{B}_0 \};\\
\mathbb{V}_{\mathbf{C}} &= \{\mathbf{C} : \mathcal{B}_0 \times \mathcal{I} \to \mathbb{S} \mid \text{ for } C_{ij} \in \mathbb{L}_2(\mathcal{B}_0) \};\\
\mathbb{V}_{\mathbf{G}} &= \{\mathbf{G} : \mathcal{B}_0 \times \mathcal{I} \to \mathbb{S} \mid \text{ for } G_{ij} \in \mathbb{L}_2(\mathcal{B}_0) \};\\
\mathbb{V}_{C} &= \{C : \mathcal{B}_0 \times \mathcal{I} \to \mathbb{R} \mid \text{ for } C \in \mathbb{L}_2(\mathcal{B}_0) \}.
\end{aligned} \tag{17}$$

Here, H^1 denotes the space of functions with square integrable first derivatives, $\mathbb{L}_2$ denotes the space of square integrable functions and $\mathbb{S}$ is the vector space of symmetric second-order tensors. Note that the symmetry condition implies that $\dim(\mathbb{S}) = 6$. Correspondingly, the constraints (16) comprise 13 independent algebraic equations. Moreover, the spaces of admissible electrical potential and electrical displacement field are provided by

$$\begin{aligned}
\mathcal{C}_{\phi} &= \{\phi : \mathcal{B}_0 \times \mathcal{I} \to \mathbb{R} \mid \text{ for } \phi \in H^1(\mathcal{B}_0),\; \phi = \bar{\phi} \;\forall \mathbf{X} \in \partial_{\phi}\mathcal{B}_0 \};\\
\mathbb{V}_{\boldsymbol{D}} &= \{\mathbf{D} : \mathcal{B}_0 \times \mathcal{I} \to \mathbb{R}^3 \mid \text{ for } D_i \in \mathbb{L}_2(\mathcal{B}_0) \}.
\end{aligned} \tag{18}$$

Next, we define a mixed variational formulation suitable for electromechanics. Therefore, we make use of a mixture of both, the electro-mechanical formulation inspired by the framework of polyconvex internal energies given in [1] and the extension to a cascade mixed formulation as provided by [2]. The newly proposed variational formulation relies on the following 9-field functional of the Hu-Washizu type:

$$\begin{aligned}
\Pi(\boldsymbol{\varphi}, \boldsymbol{\Xi}, \boldsymbol{\Lambda}, \phi, \mathbf{D}) = \int_{\mathcal{B}_0} \mathbb{U}(\mathbf{C}, \mathbf{G}, C, \mathbf{D})\,\mathrm{d}V &+ \int_{\mathcal{B}_0} \boldsymbol{\Lambda}^{\mathbf{C}} : (\nabla\boldsymbol{\varphi}^{\mathrm{T}}\nabla\boldsymbol{\varphi} - \mathbf{C})\,\mathrm{d}V\\
&+ \int_{\mathcal{B}_0} \boldsymbol{\Lambda}^{\mathbf{G}} : \Big(\frac{1}{2}\mathbf{C} \,\#\, \mathbf{C} - \mathbf{G}\Big)\,\mathrm{d}V\\
&+ \int_{\mathcal{B}_0} \Lambda^{C} \Big(\frac{1}{3}\mathbf{C} : \mathbf{G} - C\Big)\,\mathrm{d}V\\
&+ \int_{\mathcal{B}_0} \mathbf{D} \cdot \nabla\phi\,\mathrm{d}V + \Pi_{\text{ext}}(\boldsymbol{\varphi}, \phi),
\end{aligned} \tag{19}$$

where the abbreviations of the independent fields $\boldsymbol{\Xi} = (\mathbf{C}, \mathbf{G}, C)$ and $\boldsymbol{\Lambda} = (\boldsymbol{\Lambda}^{\mathbf{C}}, \boldsymbol{\Lambda}^{\mathbf{G}}, \Lambda^{C})$ have been introduced for convenience of notation. As it can be observed from the variational functional (19), the three kinematic constraints (16) are enforced by means of Lagrange multipliers $\boldsymbol{\Lambda}^{\mathbf{C}} \in \mathbb{V}_{\mathbf{C}}$, $\boldsymbol{\Lambda}^{\mathbf{G}} \in \mathbb{V}_{\mathbf{G}}$, and $\Lambda^{C} \in \mathbb{V}_{C}$. The external potential can be split into a mechanical and electrical contribution $\Pi_{\text{ext}}(\boldsymbol{\varphi}, \phi) = \Pi^{m}_{\text{ext}}(\boldsymbol{\varphi}) + \Pi^{e}_{\text{ext}}(\phi)$ defined as

$$\Pi^{m}_{\text{ext}}(\boldsymbol{\varphi}) = -\int_{\mathcal{B}} \bar{\mathbf{B}} \cdot \boldsymbol{\varphi}\, dV - \int_{\partial_{\boldsymbol{P}}\mathcal{B}_0} \bar{\mathbf{T}} \cdot \boldsymbol{\varphi}\, dA; \quad \Pi^{e}_{\text{ext}}(\phi) = \int_{\mathcal{B}_0} \rho^{e}_0 \phi\, dV + \int_{\partial_{\omega}\mathcal{B}_0} \omega^{e}_0 \varphi\, dA. \tag{20}$$

Note that $\int_{\mathcal{B}_0} \mathbf{D} \cdot \nabla\phi \, \mathrm{d}V + \Pi^e_{\text{ext}}(\phi)$ in (19) defines the Gauss law (6) as an additional constraint, enforced by the electrical potential ϕ.

Imposing the stationary conditions on the functional (19) we obtain the Euler-Lagrange equations. Stationarity with respect to the displacements $\boldsymbol{\varphi}$ yields

$$\mathrm{D}_{\boldsymbol{\varphi}}\Pi[\delta\boldsymbol{\varphi}] = \int_{\mathcal{B}_0} \boldsymbol{\Lambda}^{\mathbf{C}} : \left((\nabla\delta\boldsymbol{\varphi})^{\mathrm{T}} \nabla\boldsymbol{\varphi} + (\nabla\boldsymbol{\varphi})^{\mathrm{T}} \nabla\delta\boldsymbol{\varphi} \right) dV \; + \Pi^m_{\text{ext}}(\delta\boldsymbol{\varphi}) = 0 \,, \tag{21}$$

which represent the weak form of the balance of linear momentum. Stationarity with respect to the electrical potential ϕ and the electrical displacement field $\mathbf{D}$ yields

$$\begin{aligned} \mathrm{D}_{\phi}\Pi[\delta\phi] &= \int_{\mathcal{B}_0} \mathbf{D} \cdot \nabla\delta\phi \, dV + \Pi^e_{\text{ext}}(\delta\phi) = 0; \\ \mathrm{D}_{\mathbf{D}}\Pi[\delta\mathbf{D}] &= \int_{\mathcal{B}_0} \delta\mathbf{D} \cdot \left(\partial_{\boldsymbol{D}}\mathbb{U} + \nabla\phi \right) \, dV = 0 \,, \end{aligned} \tag{22}$$

which represent the weak form of the Gauss's law and Faraday's law, respectively. For the stationarity conditions with respect to the kinematic fields $\boldsymbol{\Xi}$ we obtain

$$\begin{aligned} \mathrm{D}_{\mathbf{C}}\Pi[\delta\mathbf{C}] &= \int_{\mathcal{B}_0} \delta\mathbf{C} : \left(\partial_{\mathbf{C}}\mathbb{U} - \boldsymbol{\Lambda}^{\mathbf{C}} + \boldsymbol{\Lambda}^{\mathbf{G}} \boldsymbol{\barwedge} \mathbf{C} + \tfrac{1}{3}\Lambda^C \, \mathbf{G} \right) \mathrm{d}V = 0; \\ \mathrm{D}_{\mathbf{G}}\Pi[\delta\mathbf{G}] &= \int_{\mathcal{B}_0} \delta\mathbf{G} : \left(\partial_{\mathbf{G}}\mathbb{U} - \boldsymbol{\Lambda}^{\mathbf{G}} + \tfrac{1}{3}\Lambda^C \, \mathbf{C} \right) \mathrm{d}V = 0; \\ \mathrm{D}_{C}\Pi[\delta C] &= \int_{\mathcal{B}_0} \delta C \left(\partial_{C}\mathbb{U} - \Lambda^C \right) \mathrm{d}V = 0 \,. \end{aligned} \tag{23}$$

Finally, stationary with respect to the Lagrange multipliers $\boldsymbol{\Lambda}$ yield

$$\begin{aligned} \mathrm{D}_{\boldsymbol{\Lambda}^{\boldsymbol{C}}}\Pi[\delta\boldsymbol{\Lambda}^{\mathbf{C}}] &= \int_{\mathcal{B}_0} \delta\boldsymbol{\Lambda}^{\mathbf{C}} : \left((\nabla\boldsymbol{\varphi})^{\mathrm{T}} \nabla\boldsymbol{\varphi} - \mathbf{C} \right) \mathrm{d}V = 0; \\ \mathrm{D}_{\boldsymbol{\Lambda}^{\boldsymbol{G}}}\Pi[\delta\boldsymbol{\Lambda}^{\mathbf{G}}] &= \int_{\mathcal{B}_0} \delta\boldsymbol{\Lambda}^{\mathbf{G}} : \left(\tfrac{1}{2}\, \mathbf{C} \boldsymbol{\barwedge} \mathbf{C} - \mathbf{G} \right) \mathrm{d}V = 0; \\ \mathrm{D}_{\Lambda^{C}}\Pi[\delta\Lambda^{C}] &= \int_{\mathcal{B}_0} \delta\Lambda^C \left(\tfrac{1}{3}\mathbf{G} : \mathbf{C} - C \right) \mathrm{d}V = 0 \,. \end{aligned} \tag{24}$$

The above equations have to hold for arbitrary $\delta\boldsymbol{\varphi} \in \mathcal{V}_{\boldsymbol{\varphi}}$, $\delta\phi \in \mathcal{V}_{\phi}$ and arbitrary $\delta\mathbf{C} \in \mathbb{V}_{\mathbf{C}}$, $\delta\mathbf{G} \in \mathbb{V}_{\mathbf{G}}$, $\delta C \in \mathbb{V}_{C}$, $\delta\boldsymbol{\Lambda}^{\mathbf{C}} \in \mathbb{V}_{\mathbf{C}}$, $\delta\boldsymbol{\Lambda}^{\mathbf{G}} \in \mathbb{V}_{\mathbf{G}}$, $\delta\Lambda^{C} \in \mathbb{V}_{C}$ and $\delta\mathbf{D} \in \mathbb{V}_{\boldsymbol{D}}$. The spaces of admissible variations of $\boldsymbol{\varphi}$ and ϕ are defined as

$$\begin{aligned} \mathcal{V}_{\boldsymbol{\varphi}} &= \{ \delta\boldsymbol{\varphi} : \mathcal{B}_0 \to \mathbb{R}^3 \mid \text{ for } \delta\varphi_i \in H^1(\mathcal{B}_0), \; \delta\boldsymbol{\varphi} = \mathbf{0} \; \forall \mathbf{X} \in \partial_{\boldsymbol{\varphi}}\mathcal{B}_0 \}; \\ \mathcal{V}_{\phi} &= \{ \delta\phi : \mathcal{B}_0 \to \mathbb{R} \mid \text{ for } \delta\phi \in H^1(\mathcal{B}_0), \; \delta\phi = 0 \; \forall \; \mathbf{X} \in \partial_{\phi}\mathcal{B}_0 \} \,. \end{aligned} \tag{25}$$

Note that (24) recover the kinematic constraints given in (16), while (23) yields the Lagrange multipliers.

3.1 Extension to dynamics

Next we deal with the extension of the mixed formulation introduced above to the elasto-dynamic regime. A field denoted by $(\bullet)_{\mathrm{t}}$ is defined at time $t \in \mathcal{I}$ (e.g. the motion of the continuum body is described by $\boldsymbol{\varphi}_{\mathrm{t}} \in \mathcal{C}_{\boldsymbol{\varphi}}$, where $\mathbf{x}(t) = \boldsymbol{\varphi}_{\mathrm{t}}(\mathbf{X})$ characterizes the position of the material point $\mathbf{X} \in \mathcal{B}_0$). Based on the local form of balance of linear momentum given in (5), we extend (21) to elastodynamics. Accordingly, (21) is replaced by

$$\begin{aligned}
&\int_{\mathcal{B}_0} \delta\mathbf{V} \cdot (\dot{\boldsymbol{\varphi}}_{\mathrm{t}} - \mathbf{V}_{\mathrm{t}})\, \rho_0 \, \mathrm{d}V = 0; \\
&\int_{\mathcal{B}_0} \left(\delta\boldsymbol{\varphi} \cdot \rho_0 \, \dot{\mathbf{V}}_{\mathrm{t}} + \boldsymbol{\Lambda}^{\mathbf{C}}_{\mathrm{t}} : \left((\nabla\delta\boldsymbol{\varphi})^{\mathrm{T}} \nabla\boldsymbol{\varphi}_{\mathrm{t}} + (\nabla\boldsymbol{\varphi}_{\mathrm{t}})^{\mathrm{T}} \nabla\delta\boldsymbol{\varphi}\right) \mathrm{d}V + \Pi^{\mathrm{ext}}_m(\delta\boldsymbol{\varphi}) = 0\,,
\end{aligned} \tag{26}$$

while the variational equations (22)-(24) remain the same. The variational equations have to hold for arbitrary $\{\delta\boldsymbol{\varphi}, \delta\mathbf{V}, \delta\mathbf{C}, \delta\mathbf{G}, \delta C, \delta\boldsymbol{\Lambda}^{\mathbf{C}}, \delta\boldsymbol{\Lambda}^{\mathbf{G}}, \delta\Lambda^{C}, \delta\phi, \delta\mathbf{D}\} \in \mathcal{V}_{\boldsymbol{\varphi}} \times \mathcal{V}_{\boldsymbol{\varphi}} \times \mathbb{V}_{\mathbf{C}} \times \mathbb{V}_{\mathbf{G}} \times \mathbb{V}_{C} \times \mathbb{V}_{\mathbf{C}} \times \mathbb{V}_{\mathbf{G}} \times \mathbb{V}_{C} \times \mathcal{V}_{\phi} \times \mathbb{V}_{\mathbf{D}}$ and be supplemented by prescribed initial values $\boldsymbol{\varphi}_0 \in \mathcal{V}_{\boldsymbol{\varphi}}$, $\mathbf{V}_0 \in \mathcal{V}_{\boldsymbol{\varphi}}$ and $\phi_0 \in \mathcal{V}_{\phi}$ at time $t = 0$. Consistent initial values for the mixed strain fields, $(\mathbf{C}_0, \mathbf{G}_0, C_0)$, and the electrical displacement vector $\mathbf{D}_0$ can be calculated with the use of $(22)_1$ and (23).

4 Discretization in time

Next we deal with the structure-preserving discretization in time of the mixed variational formulation presented in the previous section. We focus on a representative time interval $[t_n, t_{n+1}]$ with corresponding time-step size $\Delta t = t_{n+1} - t_n$. The discrete approximations at times t_n and t_{n+1} of the continuous variable $(\bullet)_{\mathrm{t}}$ will be denoted by $(\bullet)_n$ and $(\bullet)_{n+1}$, respectively. The average value of $(\bullet)_{\mathrm{t}}$ in the time interval $[t_n, t_{n+1}]$ is denoted by $(\bullet)_{n+\frac{1}{2}} = \frac{1}{2}\left((\bullet)_n + (\bullet)_{n+1}\right)$. Assume that the state variables $(\boldsymbol{\varphi}_n, \mathbf{V}_n, \phi_n) \in \mathcal{C}_{\boldsymbol{\varphi}} \times \mathcal{V}_{\boldsymbol{\varphi}} \times \mathcal{C}_{\phi}$ along with consistent strain variables $(\mathbf{C}_n, \mathbf{G}_n, C_n)$ and the electrical displacement field $\mathbf{D}_n$ are given. Now the semi-discrete version of the dynamical extended variational equations (26) along with (22)-(24), is introduced as

$$\begin{aligned}
&\int_{\mathcal{B}_0} \delta\mathbf{V} \cdot \tfrac{1}{\Delta t}\left(\boldsymbol{\varphi}_{n+1} - \boldsymbol{\varphi}_n\right) \rho_0 \, \mathrm{d}V = \int_{\mathcal{B}_0} \delta\mathbf{V} \cdot \mathbf{V}_{n+\frac{1}{2}} \, \rho_0 \, \mathrm{d}V; \\
&\int_{\mathcal{B}_0} \delta\boldsymbol{\varphi} \cdot \tfrac{\rho_0}{\Delta t}\left(\mathbf{V}_{n+1} - \mathbf{V}_n\right) + \boldsymbol{\Lambda}^{\mathbf{C}}_{n+1} : \left((\nabla\delta\boldsymbol{\varphi})^{\mathrm{T}} \nabla\boldsymbol{\varphi}_{n+\frac{1}{2}} + (\nabla\boldsymbol{\varphi}_{n+\frac{1}{2}})^{\mathrm{T}} \nabla\delta\boldsymbol{\varphi}\right) \mathrm{d}V = -\Pi^{m}_{\mathrm{ext}}(\delta\boldsymbol{\varphi})\Big|_{\mathrm{n}+\frac{1}{2}}; \\
&\int_{\mathcal{B}_0} \mathbf{D}_{n+\frac{1}{2}} \cdot \nabla\delta\phi \, dV = -\Pi^{e}_{\mathrm{ext}}(\delta\phi)\Big|_{n+\frac{1}{2}}; \\
&\int_{\mathcal{B}_0} \delta\mathbf{D} \cdot \left(\mathrm{D}_{\boldsymbol{D}}\mathbb{U} + \nabla\phi_{n+\frac{1}{2}}\right) dV = 0\,,
\end{aligned} \tag{27}$$

for arbitrary $\{\delta\mathbf{V}, \delta\boldsymbol{\varphi}, \delta\phi, \delta\mathbf{D}\} \in \mathcal{V}_{\boldsymbol{\varphi}} \times \mathcal{V}_{\boldsymbol{\varphi}} \times \mathcal{V}_{\phi} \times \mathbb{V}_{\boldsymbol{D}}$, together with

$$\begin{aligned}
&\int_{\mathcal{B}_0} \delta\mathbf{C} : \left(\mathrm{D}_{\mathbf{C}}\mathbb{U} - \boldsymbol{\Lambda}^{\mathbf{C}}_{n+1} + \boldsymbol{\Lambda}^{\mathbf{G}}_{n+1} \maltese \mathbf{C}_{n+\frac{1}{2}} + \tfrac{1}{3}\,\Lambda^{C}_{n+1}\,\mathbf{G}_{n+\frac{1}{2}}\right) \mathrm{d}V = 0;\\
&\int_{\mathcal{B}_0} \delta\mathbf{G} : \left(\mathrm{D}_{\mathbf{G}}\mathbb{U} - \boldsymbol{\Lambda}^{\mathbf{G}}_{n+1} + \tfrac{1}{3}\Lambda^{C}_{n+1}\,\mathbf{C}_{n+\frac{1}{2}}\right) \mathrm{d}V = 0;\\
&\int_{\mathcal{B}_0} \delta C \left(\mathrm{D}_{C}\mathbb{U} - \Lambda^{C}{}_{n+1}\right) \mathrm{d}V = 0;\\
&\int_{\mathcal{B}_0} \delta\boldsymbol{\Lambda}^{\mathbf{C}} : \left((\nabla\boldsymbol{\varphi}_{n+1})^{\mathrm{T}}\nabla\boldsymbol{\varphi}_{n+1} - \mathbf{C}_{n+1}\right) \mathrm{d}V = 0;\\
&\int_{\mathcal{B}_0} \delta\boldsymbol{\Lambda}^{\mathbf{G}} : \left(\tfrac{1}{2}\,\mathbf{C}_{n+1} \maltese \mathbf{C}_{n+1} - \mathbf{G}_{n+1}\right) \mathrm{d}V = 0;\\
&\int_{\mathcal{B}_0} \delta\Lambda^{C} \left(\tfrac{1}{3}\mathbf{G}_{n+1} : \mathbf{C}_{n+1} - C_{n+1}\right) \mathrm{d}V = 0\,,
\end{aligned} \tag{28}$$

for arbitrary $\{\delta\mathbf{C}, \delta\mathbf{G}, \delta C, \delta\boldsymbol{\Lambda}^{\mathbf{C}}, \delta\boldsymbol{\Lambda}^{\mathbf{G}}, \delta\Lambda^{C}\} \in \mathbb{V}_{\mathbf{C}} \times \mathbb{V}_{\mathbf{G}} \times \mathbb{V}_{C} \times \mathbb{V}_{\mathbf{C}} \times \mathbb{V}_{\mathbf{G}} \times \mathbb{V}_{C}$. Moreover, in $(27)_4$ and $(28)_{1\text{–}3}$, the time-discrete versions of the partial derivatives of the internal energy $(\partial_{\mathbf{C}}\mathbb{U}, \partial_{\mathbf{G}}\mathbb{U}, \partial_{C}\mathbb{U}, \partial_{\boldsymbol{D}}\mathbb{U})$ are replaced by $(\mathrm{D}_{\mathbf{C}}\mathbb{U}, \mathrm{D}_{\mathbf{G}}\mathbb{U}, \mathrm{D}_{C}\mathbb{U}, \mathrm{D}_{\boldsymbol{D}}\mathbb{U})$. In particular, we assume that $(\mathrm{D}_{\mathbf{C}}\mathbb{U}, \mathrm{D}_{\mathbf{G}}\mathbb{U}, \mathrm{D}_{C}\mathbb{U}, \mathrm{D}_{\boldsymbol{D}}\mathbb{U})$ are partitioned discrete derivatives in the sense of [3] for the internal energy density $\mathbb{U}(\mathbf{C}, \mathbf{G}, C, \mathbf{D})$. For the specific definition of the partitioned discrete derivative in the context of the underlying electro-elastodynamic problem, see [4]. Accordingly, the following property is assumed to be satisfied by definition of the discrete derivatives for the internal energy:

$$\begin{aligned}
&\mathbb{U}(\mathbf{C}_{n+1}, \mathbf{G}_{n+1}, C_{n+1}, \mathbf{D}_{n+1}) - \mathbb{U}(\mathbf{C}_{n}, \mathbf{G}_{n}, C_{n}, \mathbf{D}_{n})\\
&= \mathrm{D}_{\mathbf{C}}\mathbb{U} : (\mathbf{C}_{n+1} - \mathbf{C}_{n}) + \mathrm{D}_{\mathbf{G}}\mathbb{U} : (\mathbf{G}_{n+1} - \mathbf{G}_{n}) + \mathrm{D}_{C}\mathbb{U}(C_{n+1} - C_{n}) + \mathrm{D}_{\boldsymbol{D}}\mathbb{U} \cdot (\mathbf{D}_{n+1} - \mathbf{D}_{n})\,.
\end{aligned} \tag{29}$$

This property yields an energy consistent time integration scheme for the proposed electro-mechanical system, see [2, 4].

5 Discretization in space

For the discretisation in space we apply standard isoparametric finite elements based on finite-dimensional approximations $\{\boldsymbol{\varphi}^{\mathrm{h}}_{\mathrm{t}}, \mathbf{V}^{\mathrm{h}}_{\mathrm{t}}, \phi^{\mathrm{h}}_{\mathrm{t}}, \mathbf{D}^{\mathrm{h}}_{\mathrm{t}}\} \in \mathcal{C}^{\mathrm{h}}_{\boldsymbol{\varphi}} \times \mathcal{V}^{\mathrm{h}}_{\boldsymbol{\varphi}} \times \mathcal{C}^{\mathrm{h}}_{\phi} \times \mathbb{V}^{\mathrm{h}}_{\boldsymbol{D}} \subset \mathcal{C}_{\boldsymbol{\varphi}} \times \mathcal{V}_{\boldsymbol{\varphi}} \times \mathcal{C}_{\phi} \times \mathbb{V}_{\boldsymbol{D}}$ of the form

$$\begin{aligned}
&\mathcal{C}^{\mathrm{h}}_{\boldsymbol{\varphi}} = \{\boldsymbol{\varphi}_{\mathrm{t}} \in \mathcal{C}_{\boldsymbol{\varphi}} \mid \boldsymbol{\varphi}^{\mathrm{h}}_{\mathrm{t}}\Big|_{\mathcal{B}^{\mathrm{e}}_0} = \sum_{a=1}^{n_{\mathrm{node}}} N^{\boldsymbol{\varphi}}_{a}\,\boldsymbol{\varphi}^{a}_{\mathrm{t}}\ \};\ \mathcal{V}^{\mathrm{h}}_{\boldsymbol{V}} = \{\boldsymbol{\varphi}_{\mathrm{t}} \in \mathcal{V}_{\boldsymbol{\varphi}} \mid \mathbf{V}^{\mathrm{h}}_{\mathrm{t}}\Big|_{\mathcal{B}^{\mathrm{e}}_0} = \sum_{a=1}^{n_{\mathrm{node}}} N^{\boldsymbol{V}}_{a}\,\mathbf{V}^{a}_{\mathrm{t}}\ \}\\
&\mathcal{C}^{\mathrm{h}}_{\phi} = \{\phi_{\mathrm{t}} \in \mathcal{C}_{\phi} \mid \phi^{\mathrm{h}}_{\mathrm{t}}\Big|_{\mathcal{B}^{\mathrm{e}}_0} = \sum_{a=1}^{n_{\mathrm{node}}} N^{\phi}_{a}\,\phi^{a}_{\mathrm{t}}\ \};\ \mathbb{V}^{\mathrm{h}}_{\boldsymbol{D}} = \{\mathbf{D}_{\mathrm{t}} \in \mathbb{V}_{\boldsymbol{D}} \mid \mathbf{D}^{\mathrm{h}}_{\mathrm{t}}\Big|_{\mathcal{B}^{\mathrm{e}}_0} = \sum_{b=1}^{n_{\mathrm{node}}} M^{\boldsymbol{D}}_{b}\,\mathbf{D}^{b}_{\mathrm{t}}\ \}\,.
\end{aligned} \tag{30}$$

Here, $N_a^\bullet : \mathcal{B}_0 \to \mathbb{R}$ with $a = 1, ..., n_{\text{node}}$ denotes the nodal shape functions and $(\bullet)_{\text{t}}^a$ are the respective nodal values at time t. Here, n_{node} denotes the total number of nodes in the finite element mesh. Moreover, the strain variables $\mathbf{C}_{\text{t}}^{\text{h}}, \mathbf{G}_{\text{t}}^{\text{h}}, C_{\text{t}}^{\text{h}}$ and the Lagrange multipliers $\mathbf{\Lambda}_{\text{t}}^{\mathbf{C}^{\text{h}}}, \mathbf{\Lambda}_{\text{t}}^{\mathbf{G}^{\text{h}}}, \Lambda_{\text{t}}^{C^{\text{h}}}$ are based on approximations $\mathbb{V}_{\boldsymbol{C}}, \mathbb{V}_{\boldsymbol{G}}, \mathbb{V}_C$ of the form

$$\mathbb{V}_{\mathbf{A}}^{\text{h}} = \{ \mathbf{A}_{\text{t}} \in \mathbb{V}_{\mathbf{A}} \mid \mathbf{A}_{\text{t}}^{\text{h}} \big|_{\mathcal{B}_0^e} = \sum_{b=1}^{n_{\text{node}}} M_b^{\boldsymbol{A}} \, \mathbf{A}_{\text{t}}^b, \ (\mathbf{A}_{\text{t}}^b = \mathbf{A}_{\text{t}}^{b^{\text{T}}}) \ \} . \tag{31}$$

where $\mathbf{A}$ stands for the second-order tensors $\mathbf{C}$, $\mathbf{G}$, $\mathbf{\Lambda}^{\mathbf{C}}$, $\mathbf{\Lambda}^{\mathbf{G}}$ or scalars C, Λ^C. Accordingly, the present sample application relies on uniform element-wise approximations for the strains, the Lagrange multipliers and the electrical displacement field making use of the shape functions $M_b^\bullet : \mathcal{B}_0 \to \mathbb{R}$, with $b = 1, ..., n_{\text{node}}$. The standard (Bubnov) Galerkin approach relies on analogous approximations for the corresponding variations. Since no inter-element continuity is required for the mixed approximations (related to the shape functions $M_b^\bullet$), the additional unknowns can be eliminated on element level, see [1, 2]. Moreover, the proposed discretization in space does not affect the EM scheme and inherits the fundamental balance laws.

6 Numerical example

The goal of this numerical example, depicted in Fig. 1, is to verify the conservation properties of the newly proposed EM method.

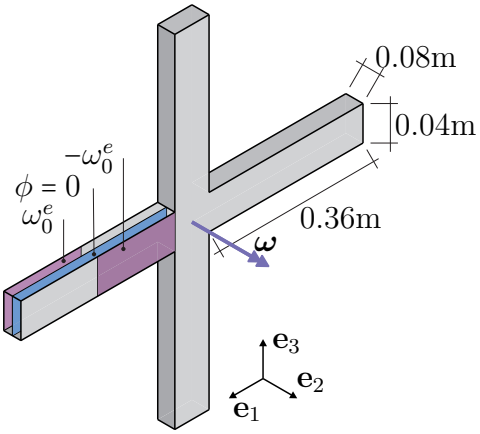

Figure 1: Rotating cross-shaped body with electrical boundary conditions

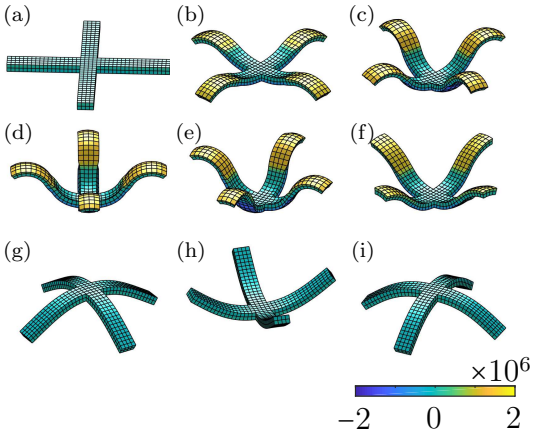

Figure 2: Snapshots with electrical potential distribution at $t = \{0, 0.2, 0.3, 0.4, 0.6, 3.2, 3.5, 3.7, 4\}\, s$

We use the internal energy given in (14)-(15) where the material parameters are $\mu_1 = 5 \times 10^4\,\text{Pa}$, $\mu_2 = 1 \times 10^5\,\text{Pa}$, $\lambda = 5 \times 10^5\,\text{Pa}$, $\varepsilon_0 = 8.854 \times 10^{-12}\,\text{A}^2\,\text{s}^4\,\text{kg}^{-1}\,\text{m}^{-3}$, $\varepsilon_r = 4$ with reference density of $\rho_0 = 1000\,\text{kg}\,\text{m}^{-3}$. There are no mechanical Dirichlet

boundary conditions and the initial velocity is assumed to be $\mathbf{V}_0 = \boldsymbol{\omega} \times \mathbf{X}$, with $\boldsymbol{\omega} = [0, 0, 4]^T\, s^{-1}$. On the blue electrode, a constant value of $\phi = 0\,\mathrm{V}$ is applied. On the purple electrode a time dependent electrical surface charge ω_0^e is applied, where the time dependent function of ω_0^e is given by $\omega_0^e = 5 \cdot 10^{-3} \cdot \sin(\frac{0.5\,\pi}{0.4\,\mathrm{s}}\, t)$ for $t \leq 0.4\,\mathrm{s}$, $\omega_0^e = 5 \cdot 10^{-3}$ for $0.4\,\mathrm{s} < t \leq 3.0\,\mathrm{s}$, $\omega_0^e = 5 \cdot 10^{-3} \cdot \cos(\frac{0.5\,\pi}{3.4\,\mathrm{s} - 3.0\,\mathrm{s}}\,(t - 3\,\mathrm{s}))$ for $3.0\,\mathrm{s} < t \leq 3.4\,\mathrm{s}$ and $\omega_0^e = 0$ for $t > 3.4\,\mathrm{s}$. Note that the cross-shaped body has the same boundary conditions and dimensions in each wing. For the spatial discretization, we use a total of 672 hexahedral finite elements with continuous quadratic (20-nodes Serendepity type interpolation) Ansatz for $\boldsymbol{\varphi}_\mathrm{t}^\mathrm{h}, \mathbf{V}_\mathrm{t}^\mathrm{h}, \phi_\mathrm{t}^\mathrm{h}$ and a discontinuous linear (8-node) Ansatz for the other fields. The time-step size is $\Delta t = 0.01\,\mathrm{s}$ and the simulation time $T = 10\,\mathrm{s}$.

The total angular momentum is defined by $\mathbf{J} = \int_{\mathcal{B}_0} \boldsymbol{\varphi} \times \rho_0\, \mathbf{V}\, dV$ and the total Hamiltonian is given by $\mathcal{H} = \int_{\mathcal{B}_0} \frac{1}{2} \rho_0 \mathbf{V} \cdot \mathbf{V}\, dV + \int_{\mathcal{B}_0} \mathbb{U}\,(\mathbf{C}, \mathbf{G}, C, \mathbf{D})\, dV + \int_{\mathcal{B}_0} \mathbf{D} \cdot \nabla \phi\, dV + \Pi_\mathrm{ext}\,(\boldsymbol{\varphi}, \phi)$. It can be easily verified in an analytically way, that the proposed scheme consistently approximates the discrete versions of $\mathbf{J}$ and $\mathcal{H}$, respectively (see [2, 4]). As expected, the EM scheme is capable to correctly approximate these quantities in the numerical examples as well, see Fig. 3 and Fig. 4. It is well-known that standard time-stepping schemes such that the mid-point (MP) rule show a tendency to numerical instabilities in nonlinear applications. The unstable behavior of the mid-point rule leads to a termination of the simulation after about 5 seconds. In contrast to that, the present EM scheme is numerically stable. Finally, several snapshots of the deformed cross-shaped body are plotted in Fig. 2 where the EM consistent integrator has been used.

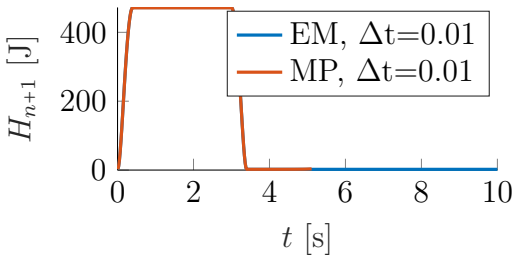

Figure 3: Time evolution of $\mathcal{H}$.

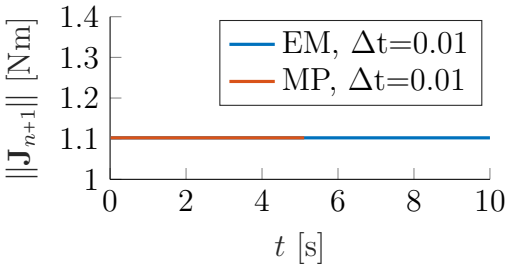

Figure 4: Time evolution of $\|\mathbf{J}\|$.

7 Conclusions

A new consistent energy-momentum one-step time integrator scheme is presented in the context of nonlinear electro-elastodynamics. The proposed schemes shows the typical advantages for the structure-preserving discretization in time. Furthermore, the mixed formulation offers several options for the discretization in space.

Acknowledgment

Support for this research was provided by the Deutsche Forschungsgemeinschaft (DFG) under Grant BE 2285/9-2. This support is gratefully acknowledged.

References

[1] A.J. Gil, and R. Ortigosa. A new framework for large strain electromechanics based on convex multi-variable strain energies: variational formulation and material characterisation. *Comput. Methods Appl. Mech. Engrg.*, 302:293–328, 2016.

[2] P. Betsch, A. Janz, and C. Hesch. A mixed variational framework for the design of energy-momentum schemes inspired by the structure of polyconvex stored energy functions. *Online in Comput. Methods Appl. Mech. Engrg.*, 2018. https://doi.org/10.1016/j.cma.2018.01.013.

[3] O. Gonzalez. Exact energy and momentum conserving algorithms for general models in nonlinear elasticity. *Comput. Methods Appl. Mech. Engrg.*, 190:1763–1783, 2000.

[4] R. Ortigosa, M. Franke, A. Janz, A.J. Gil and P. Betsch. An energy-momentum time integration scheme based on a convex multi-variable framework for nonlinear electro-elastodynamics. *Submitted to Comput. Methods Appl. Mech. Engrg.*, 2018.

[5] M. Franke, A. Janz, M. Schiebl and P. Betsch. An energy-momentum consistent integration scheme using a polyconvexity-based framework for non-linear thermo-elastodynamics. *Accepted in Int. J. Numer. Meth. Engng*, 2018.

[6] R.W. Ogden and L. Dorfmann. Nonlinear Theory of Electroelastic and Magnetoelastic Interactions. *Springer Science+Business Media*, New York, 2014.

[7] R. de Boer. Vektor- und Tensorrechnung für Ingenieure. *Springer-Verlag*, Berlin, 1982.

[8] J. Bonet, A.J. Gil, and R. Ortigosa. A computational framework for polyconvex large strain elasticity. *Comput. Methods Appl. Mech. Engrg.*, 283:1061–1094, 2015.

[9] D. K. Vu, P. Steinmann, and G. Possart. Numerical modelling of non-linear electroelasticity. *Int. J. Numer. Meth. Engng*, 70(6):685–704, 2007.